Single and multinucleon transfer in $^{19}F, ^{16}O, ^{12}C + ^{232}Th$ reactions at near barrier energies

D. C. Biswas, R. K. Choudhury, B. K. Nayak, and D. M. Nadkarni
Nuclear Physics Division, Bhabha Atomic Research Centre, Mumbai 400 085, India

V. S. Ramamurthy
Department of Science and Technology, New Delhi 110 016, India

(Received 27 December 1996)

Cross sections for single ($1p$) and multinucleon ($2p$, ^{4}He, and p^4He) transfer reactions have been measured in ^{19}F, ^{16}O, $^{12}C + ^{232}$Th systems at beam energies around the Coulomb barrier. Angular distributions and energy spectra of the projectilelike particles exhibit characteristics of direct transfer reactions. The ratio of the transfer to total reaction (transfer+fusion-fission) cross section is observed to be significantly smaller for the ^{12}C projectile, as compared to that for ^{19}F and ^{16}O projectiles. All the systems show large transfer cross sections relative to the total reaction cross section at subbarrier energies. The angular distribution data were analyzed in terms of transfer probabilities to derive the slope parameter (α) for the stripping of $1p$ and $2p$ in the case of ^{16}O and ^{12}C projectiles and for $1p$, ^{4}He and correlated (p^4He) stripping in the case of ^{19}F projectile, for comparison with the semiclassical calculations. It is observed that the semiclassical picture is valid for $1p$ transfer at energies near the Coulomb barrier, whereas for correlated $2p$, ^{4}He, and (p^4He) multinucleon transfers, the experimental values of α are anomalously small as compared to the semiclassical calculations even at subbarrier energies. At the above-barrier energies, the slope anomaly can be explained after inclusion of the nuclear effects in semiclassical calculations. [S0556-2813(97)03310-4]

PACS number(s): 25.70.Hi, 25.70.Pq

I. INTRODUCTION

In heavy ion reactions at near barrier energies, there is a strong coupling of inelastic and transfer channels to fusion reactions and thus a detailed understanding of the heavy ion reaction dynamics requires, a systematic and simultaneous study of the different reaction channels as a function of the bombarding energy [1]. In recent years there has been a lot of interest to study transfer reactions in nucleus-nucleus interactions at energies near the Coulomb barrier, due to the observation of anomalous slopes in the semiclassical description of the collision processes [2–4]. Multinucleon transfer reactions can take place due to either the one-step process or due to the cumulative effect of many possible final channels, and thus the complexity of the reaction increases with the number of transferred nucleons [5–7]. The direct reaction models such as distorted wave Born approximation (DWBA), have been successfully used in explaining the transfer cross section data and angular distribution of transfer reactions to specific final states [8]. However, in the case of transfers leading to continuum states such calculations are difficult as one has to sum over the whole spectrum of final states. Another important aspect of transfer reactions is the interference between one-step transfers, leading directly from the initial to the final states of the fragments, and multistep transfers, where the reaction proceeds sequentially through a number of inelastic transfer or excitation processes. This effect is especially pronounced where the direct route is suppressed due to small overlap between initial and final states, and indirect transitions can proceed via low lying collective states. In these cases it is found that DWBA theory is not adequate because the reaction can take place in several different ways involving successive excitation and deexcitation of the target or residual nucleus. Multistep direct reaction (MSDR) theory has been successfully applied to describe the continuum spectra in transfer reactions [9,10].

Phenomenological models based on the semiclassical approximations have been used at near barrier energies, where transfer of nucleons at large impact parameters can be described as tunneling through a potential barrier. In the semiclassical approximation the transfer probability has an exponential dependence on the distance of closest approach, D between the two interacting nuclei, i.e., $P_{\rm tr} \propto \exp(-2\alpha D)$ [11], where the transfer form factor $\alpha = \sqrt{2\mu E_b}/\hbar$; μ is the reduced mass and E_b is the effective binding energy of the transferred nucleons. D is normally calculated using the Coulomb trajectories as a function of the impact parameter or the scattering angle θ. The exponential dependence of $P_{\rm tr}$ on D is a characteristic property of the tunneling process in the transfer reactions. For one-nucleon transfer, if the transfer probability has a slope parameter α_{1N}, then the two-nucleon transfer probability is expected to fall approximately twice as steeply as the one nucleon transfer, i.e., $\alpha_{2N} \simeq 2\alpha_{1N}$. This relation holds whether the two nucleons are transferred in a sequential or correlated manner, since the two-nucleon binding energy is not very different from twice that of one nucleon (assuming the pairing energy to be small compared to $2E_b$) and the mass of the correlated pair is twice that of one nucleon. Experimentally it is observed that in many reactions the slope parameter for two nucleon transfer is very much less than expected and this effect is commonly known as the ''slope anomaly'' in the transfer reactions [12,13].

Vigezzi and Winther [14] showed that inclusion of nuclear effect is important in the calculation of the classical deflection function in the scattering processes. They have studied the application of complex trajectories to direct heavy ion reactions on the basis of semiclassical theory. Us-

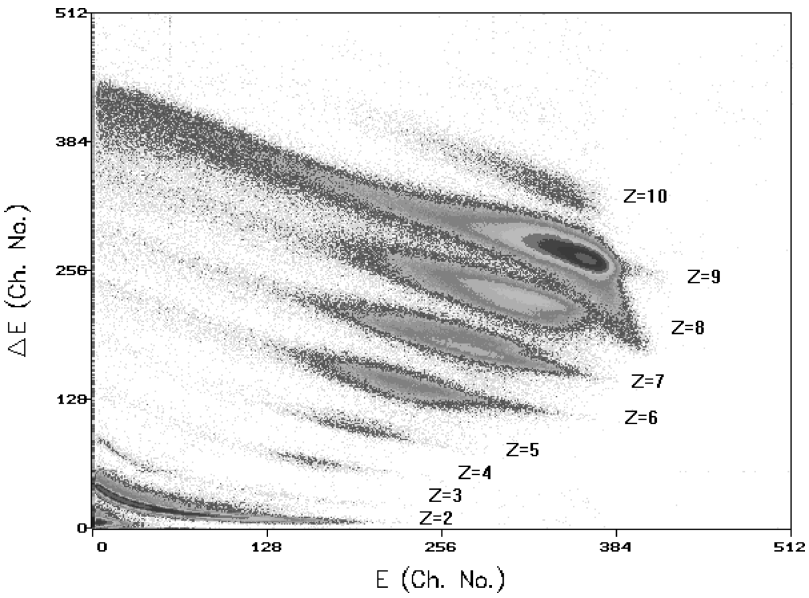

FIG. 1. E vs ΔE plot of projectilelike particles at 106.5 MeV in the $^{19}F+^{232}Th$ reaction at 100°.

ing the same formalism, Baba *et al.* [15] have recently shown that the so-called slope anomaly can be understood if the contribution from the ''nuclear branch'' of the classical deflection function is included in the calculation of transfer probability. They showed that the variation of the one- and two-nucleon transfer probability with distance of closest approach can be understood on the basis of semiclassical models if contributions from the nuclear and Coulomb branches of the classical deflection function are considered. The real part of the optical potential used in their calculations was shallower with large diffuseness parameter as compared to the one suggested by Akyuz-Winther [23]. Such a large diffusenesss parameter was interpreted by them in terms of channel coupling effects and can have bearings in the analysis of the near barrier fusion cross section data.

For heavy targets, fission is one of the dominant decay modes following multinucleon transfer or compound nucleus formation. Recently, there have been observations [16] of large anomalies in fission fragment anisotropies in many systems at near and subbarrier energies as compared to the statistical model calculations implying that the entrance channel mass asymmetry plays a role in governing the heavy ion reaction dynamics. In the present work we have measured the quasielastic scattering and transfer cross sections in ^{19}F, ^{16}O, $^{12}C+^{232}Th$ reactions at energies near the Coulomb barrier. The transfer cross sections have been compared with the total reaction cross sections (transfer+fusion-fission) for these systems. The angular distribution data for various transfer channels were transformed into transfer probabilities and studied as a function of the distance of the closest approach to obtain the experimental slope parameter for the dominant transfer channels. The results have been analyzed in terms of semiclassical models with the inclusion of the contribution of the nuclear branch of the distance of the closest approach to the transfer probability.

II. DETAILS OF THE EXPERIMENTAL SETUP AND DATA ANALYSIS

The experiments were performed at the 14 MV Pelletron heavy ion accelerator facility, Mumbai. Beams of ^{19}F, ^{16}O, and ^{12}C in different energy ranges were used to bombard a self-supporting ^{232}Th target of 1.8 mg/cm^2 thickness. The detectors were placed inside a 100 cm diameter scattering chamber operated at 10^{-6} torr vacuum. The projectilelike particles (PLP's) were detected in the angular range of 40°–160° using four ΔE-E detector telescopes. Two of these telescopes were surface barrier $\Delta E(17\mu)$-$E(500\mu)$ telescopes each covering 2 msr solid angle. The other two telescopes were a gas ionization chamber having $\Delta E_{\rm gas}$ (operating with P-10 gas at about 200 torr pressure) backed by a surface barrier E detector (500μ thickness). The details of the gas detector telescopes and their performance have been discussed elsewhere [17]. A 300μ thick surface barrier detector was placed in a forward direction of 20° to monitor the elastically scattered particles. The monitor counts were used to normalize the angular distribution of PLP's for different angular settings. Absolute cross sections for different reaction channels were obtained after normalizing the data with the elastic scattering events measured at forward angles. The beam current was limited to about 30 to 50 nanoamp to eliminate the possibility of pulse pileup, especially for the forward angle measurements.

Figure 1 shows a typical two-dimensional plot of the pulse heights of ΔE and E detectors for the $^{19}F+^{232}Th$ reaction at 106.5 MeV measured at the grazing angle ($\theta_{\rm lab}=100°$). The amplifier gains were adjusted such that all the particles from $Z=2$ to $Z=10$ could be recorded into a 512×512 ΔE-E matrix. The isotopic identification was achieved using the particle identification algorithm [6]:

$$[(E+\Delta E)^b-E^b]=KM^{(b-1)}Z^2, \tag{1}$$

where K and b are constants. It was observed that the best isotope separation for all the elements is achieved with a value of $b=1.65$. The mass identification was carried out by calibrating with ^{19}F, ^{16}O, and ^{12}C elastically scattered particles. Yields of various isotopes were obtained by fitting Gaussian distributions to the particle identification spectra of different elements as shown in Fig. 2. A mass resolution $\sigma(M)$ of about 0.5 amu was achieved in the present measurements. The isotopes corresponding to projectile Z could

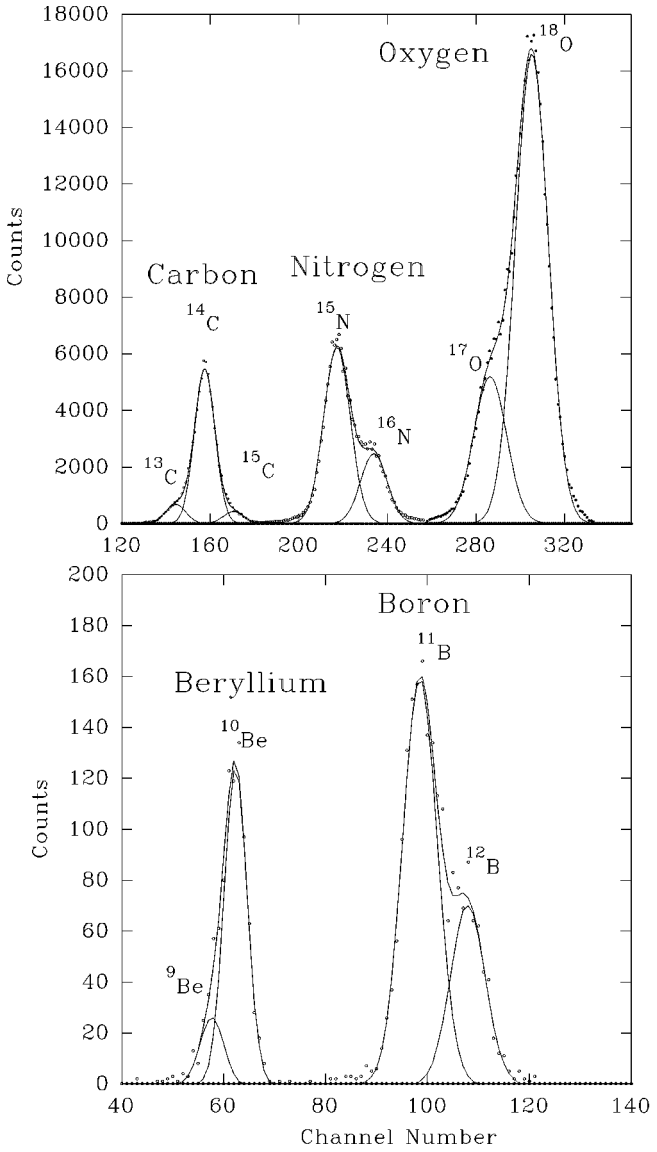

FIG. 2. PI spectrum at 100° for the $^{19}F+^{232}Th$ reaction at 106.5 MeV.

not be separated because of high counts of the elastic particles and hence the yield of neutron transfer channels are not being reported. For the $^{19}F+^{232}Th$ reaction, the dominant transfer channels are ^{18}O (corresponding to $1p$ stripping), ^{15}N (corresponding to ^{4}He transfer) and ^{14}C (corresponding to $p^{4}He$ stripping). In case of the $^{16}O+^{232}Th$ reaction, the dominant reaction channels are ^{15}N ($1p$-stripping) and ^{14}C ($2p$-stripping) and in case of $^{12}C+^{232}Th$, the dominant cross sections are again for $1p$ and $2p$ stripping channels leading to ^{11}B and ^{10}Be, respectively. In the present paper we report the analysis of the angular distributions, transfer probabilities, and slope parameters for the dominant channels for all the three systems at the near barrier energies.

III. RESULTS AND DISCUSSION

A. Energy spectra of projectilelike particles

Typical energy spectra of the projectilelike particles of different Z values produced at the grazing angle (100°) in the $^{19}F+^{232}Th$ reaction at 106.5 MeV are shown in Fig. 3. The

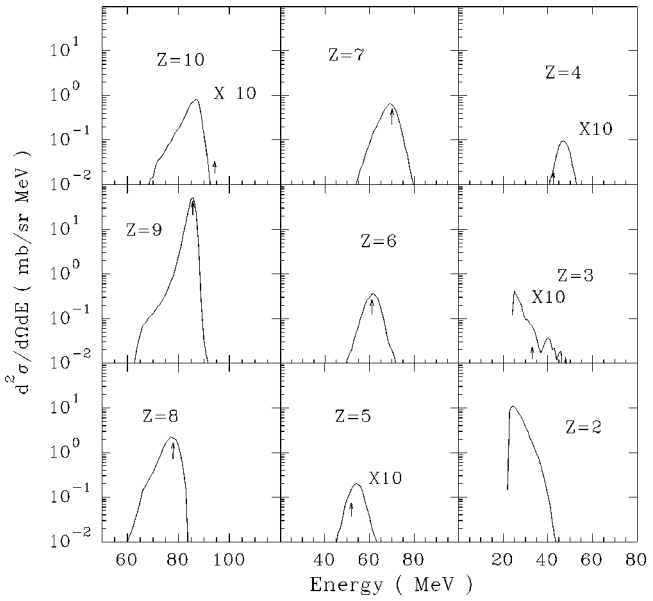

FIG. 3. Energy spectrum of projectilelike particles at 100° for the $^{19}F+^{232}Th$ reaction at 106.5 MeV.

spectra indicate the characteristic features of transfer reactions for $Z>3$. For $Z=2$ and 3, the energy spectra are mostly dominated by evaporation of these particles produced in the reaction. The peak energy corresponds to a velocity slightly lower than that of the projectile having a tendency to shift towards lower velocities as the charge of the PLP moves away from that of the projectile. The shape of the energy spectra is essentially Gaussian with a low energy tail and a width depending on the PLP charge. We have reported earlier that the transfer cross sections have strong Q-value dependence in the exit channel [6].

The energy spectra of the projectilelike particles (PLP's) have been very well described by Alhassid *et al.* [18] and Karp *et al.* [19] using the concepts of maximal entropy formalism known as surprisal analysis. In this method one fits the measured energy spectra of the exit channels with the constrained phase space approach and finds that the energy spectra follow a statistical distribution with the peak corresponding to some optimum Q value (Q_{opt}). The expression for (Q_{opt}) is given as [1]

$$Q_{opt}=[(Z_3Z_4-Z_1Z_2)/Z_1Z_2]E_i\,, \tag{2}$$

where Z_1, Z_2, Z_3, and Z_4 are the charge numbers of the projectile, target, ejectile and residual nucleus, respectively, and E_i is the bombarding energy in the center of mass system. The peak energies calculated using the Q_{opt} values have been marked as arrows in Fig. 3 for the dominant isotopes. It is seen that the peaks in the energy spectra are well described by the Q_{opt} calculated using the above expression. However for $Z\leqslant 5$, there is some deviation, which can be due to multistep processes involved in multinucleon and/or multicluster transfer.

B. Angular distribution of quasielastic scattering and projectilelike particles

The experimentally measured quasielastic (elastic +inelastic) scattering cross sections have been plotted in Fig.

4 after normalizing with the Rutherford cross section. With the given energy resolution and target thickness, the low lying inelastic excited states could not be separated from the elastically scattered particles in the present experiment, and the data therefore correspond to the broad quasielastic peak seen in the measured spectra. The angular distributions were obtained in the angular range of $\theta_{lab}=40°-160°$ for the ^{19}F, ^{16}O, $^{12}C+^{232}Th$ systems at energies around the Coulomb barrier as shown in Fig. 4. An optical model fit to the experimental data was obtained with the SNOOPY8Q code [20] assuming the Woods-Saxon form of the potential. The real and imaginary potentials are V and W, respectively, with real and imaginary radii R_0 and R_{i0} having surface diffuseness a_0 and a_i. The solid lines in Fig. 4 are the optical model fits to the data obtained with the SNOOPY8Q code. The optical model potential parameters were obtained from the best fits to the

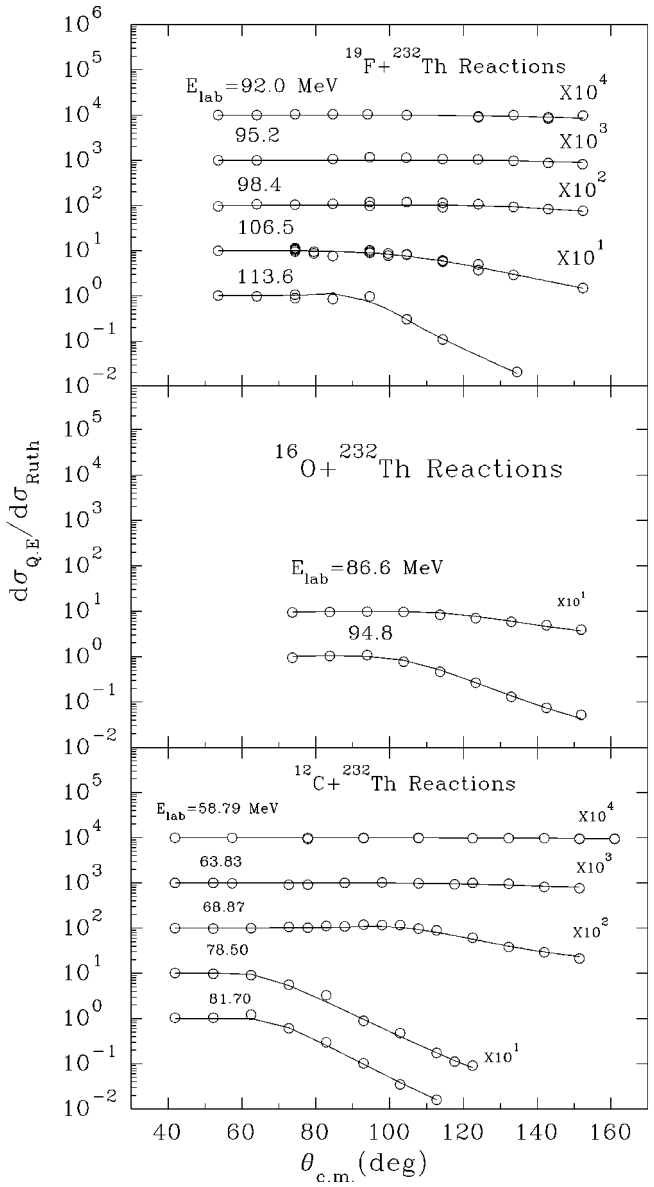

FIG. 4. The quasielastic (elastic+inelastic) scattering angular distribution normalized with Rutherford cross section data for ^{19}F, ^{16}O, $^{12}C+^{232}Th$ reactions. The solid lines are the optical model fit to the experimental data. The error bars are within the data points.

TABLE I. Optical-model parameters from fits to experimental quasielastic differential cross section data.

Systems	E_{lab} (MeV)	V (MeV)	R_0 (fm)	a (fm)	W (MeV)	R_{i0} (fm)	a_i (fm)
	113.6	40.0	1.10	0.9	19.9	1.28	0.34
	106.5	38.8	1.10	0.9	15.6	1.28	0.34
$^{19}F+^{232}Th$	98.4	45.6	1.10	0.9	10.5	1.28	0.34
	95.2	52.0	1.10	0.9	12.3	1.28	0.34
	92.0	46.5	1.10	0.9	8.6	1.28	0.34
$^{16}O+^{232}Th$	94.8	39.8	1.11	0.8	12.2	1.36	0.38
	86.6	42.2	1.11	0.8	8.3	1.36	0.38
	81.7	40.4	1.12	0.8	9.8	1.40	0.35
	78.5	41.3	1.12	0.8	10.4	1.40	0.35
$^{12}C+^{232}Th$	68.8	38.0	1.12	0.8	8.3	1.40	0.35
	63.8	39.8	1.12	0.8	9.6	1.40	0.35
	58.7	40.2	1.12	0.8	6.4	1.40	0.35

quasielastic scattering data at the highest energies for all the systems. At other energies only V and W were varied to find the best fit to the data by keeping radius and diffuseness parameters fixed. The values of the fitted parameters are listed in Table I. The primary aim of the optical model analysis was to derive the potential parameters to use them in semiclassical calculations for determination of the transfer probabilities as a function of the distance of closest approach as discussed in Sec. IV.

The energy integrated (up to 25 MeV excitation energy) cross sections of the PLP's of different Z are shown in Fig. 5 as a function of the detection angle for all the three systems at different beam energies. It is seen that the angular distributions are nearly bell-shaped and become broader with increasing nucleon transfer. As the beam energy approaches the Coulomb barrier, the grazing angle shifts towards backward angle and the distribution peaks around 180° at subbarrier energies. In case of the $^{19}F+^{232}Th$ system, the yield of oxygen (corresponding to $\Delta Z=1$) is always significantly larger in comparison to nitrogen ($\Delta Z=2$) and carbon ($\Delta Z=3$) at all energies. However, in case of $^{16}O+^{232}Th$ and $^{12}C+^{232}Th$ reactions the yield of $\Delta Z=1$ and $\Delta Z=2$ are comparable at higher energies and as the beam energy approaches the barrier energy, the cross section corresponding to $\Delta Z=1$ is found to be more than that of the $\Delta Z=2$ channel. The striking differences in the behavior of the yield of transfer channels for the various systems may be related to the structure of the projectile and entrance channel dynamics of the reactions. Another aspect in the behavior of transfer reaction cross sections for the different systems is brought out in the following section.

C. Total cross sections for transfer and fusion-fission reactions

Figure 6 shows the angle and energy integrated cross sections of the dominant transfer reaction channels measured in the present experiment as a function of the bombarding energy for all the three systems along with some of the earlier measurements on the $^{16}O+^{232}Th$ system [19,21]. In the same figure we have also plotted the earlier measurements of the fusion-fission cross sections [16]. The solid lines are

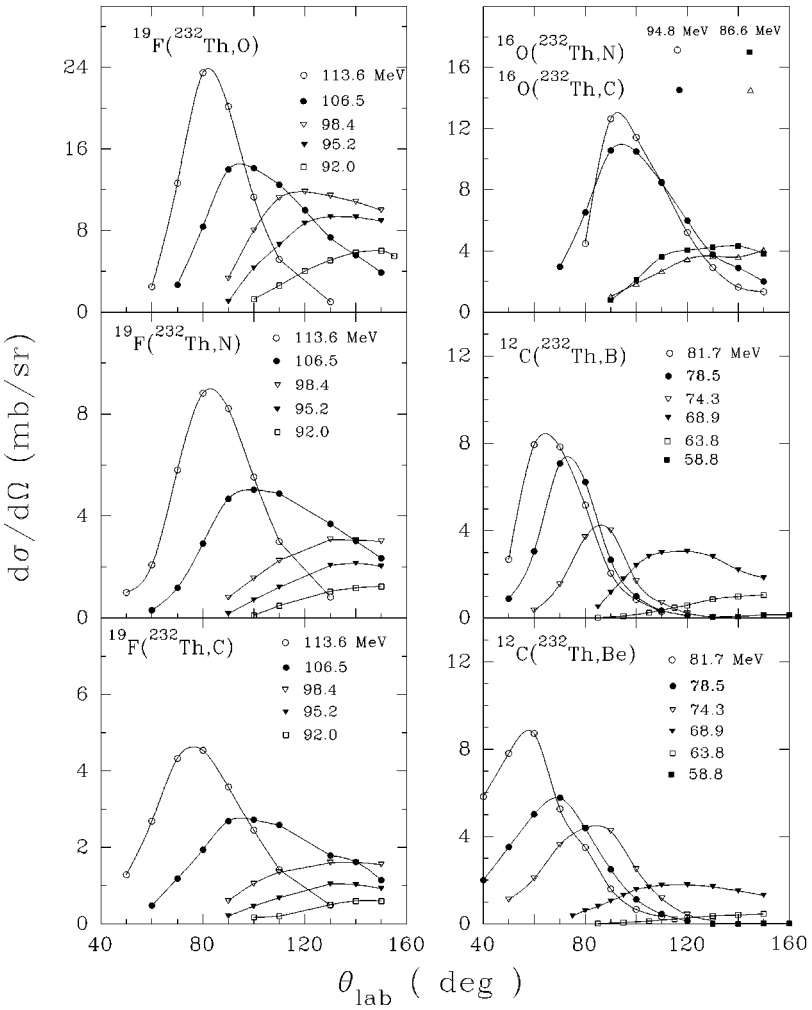

FIG. 5. Differential cross section of the dominant transfer channels in the ^{19}F, ^{16}O, ^{12}C + ^{232}Th reactions at various bombarding energies. Errors are within the data points.

theoretically calculated fusion cross sections using Wong's model [22], whereas the dashed lines are smoothly joined lines through the transfer cross section data. The total reaction cross sections can be obtained by adding the fusion-fission cross sections to the transfer cross sections. The main features that are observed from the comparison between the total cross sections for charged particle transfer channel (σ_{tr}) and fusion-fission cross sections (σ_{ff}) are the following: (i) transfer excitation functions have a much flatter energy dependence than fission excitation functions, and (ii) the transfer cross sections become dominant at subbarrier energies as compared to fusion-fission cross sections.

In Fig. 7 we have plotted the ratio of total transfer cross section (σ_{tr}) to the total reaction cross section ($\sigma_{tr}+\sigma_{ff}$) as a function of beam energy in unit of E_{cm}/V_B (where V_B is the Coulomb barrier) in all the three cases. It is seen that at energies above the Coulomb barrier, this ratio shows a saturation and at subbarrier energies it increases sharply for all the systems. The systems of ^{19}F + ^{232}Th and ^{16}O + ^{232}Th have nearly the same behavior at all energies and the transfer cross section is comparatively more enhanced in these cases than the ^{12}C + ^{232}Th system. Qualitatively, this result may indicate that in the case of the former two systems, the dinuclear system after some nucleon exchange separates more easily, as compared to the ^{12}C + ^{232}Th system. In other words the ^{12}C + ^{232}Th system is more likely to proceed to a fusion-fission channel than reseparation after nucleon transfer. However, at subbarrier energies, all the systems show enhanced transfer yields and therefore transfer reactions are expected to play an important role in the entrance channel dynamics of the reaction at these energies. These results may have a bearing on the experimental observations of entrance channel effects seen in fusion-fission angular distributions in these systems [16].

D. Semiclassical analysis of transfer probabilities

The angular distributions shown in Fig. 5 may be alternatively presented as transfer probability P_{tr} vs the distance of closest approach D. The transfer probability is obtained by taking the ratio of the transfer cross section to the corresponding Rutherford cross section, i.e.,

$$P_{tr}=(d\sigma_{tr}/d\Omega)/(d\sigma_{Ruth}/d\Omega). \tag{3}$$

The distance of closest approach is calculated under the semiclassical approximation, assuming Coulomb trajectories, as

$$D=(Z_pZ_te^2/2E_{c.m.})[1+1/\sin(\theta_{c.m.}/2)], \tag{4}$$

where Z_p and Z_t are the atomic numbers of the projectile and target, respectively. $E_{c.m.}$ and $\theta_{c.m.}$ are the beam energy and scattering angle in the c.m. system. The use of expres-

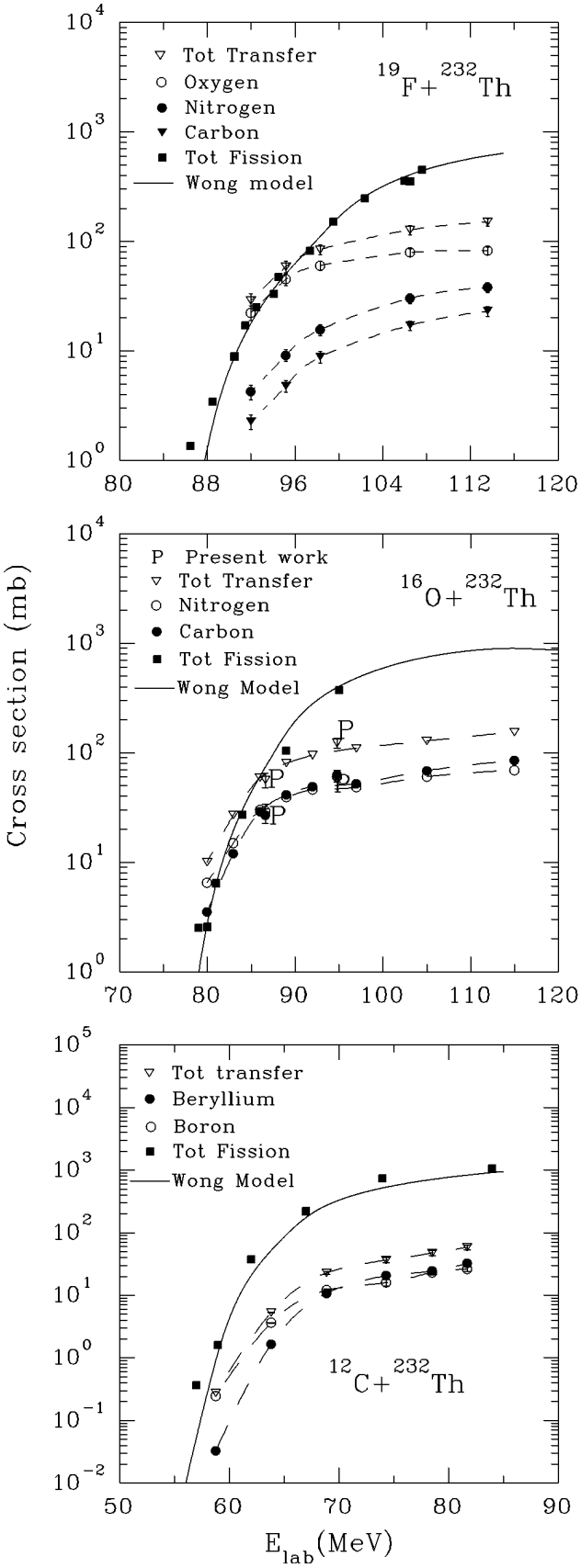

FIG. 6. Excitation function of transfer yield (the dashed lines are a guide to the eye) as well as total fission (solid lines are the Wong model calculations). The transfer data for the $^{16}O+^{232}Th$ reaction are reported from [19] and [21] along with the present work (denoted by P).

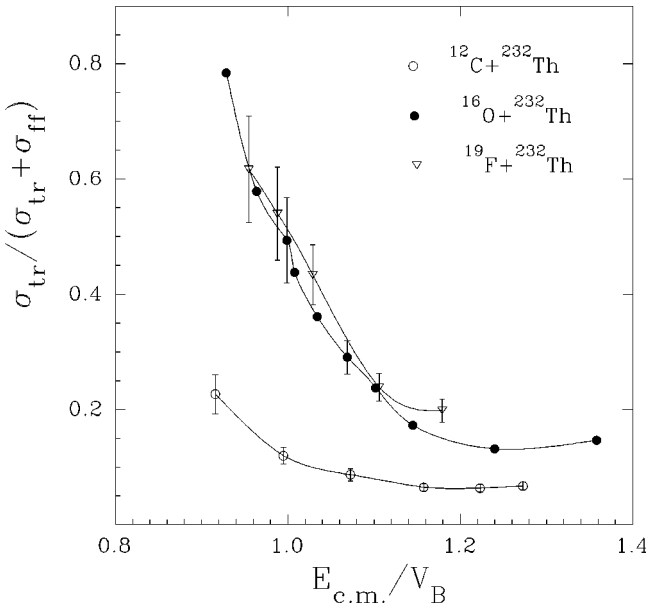

FIG. 7. Ratio of transfer cross section to the total reaction cross section plotted as a function of bombarding energies for ^{19}F, ^{16}O, $^{12}C+^{232}Th$ reactions.

ion (4) is justified for peripheral reactions since only small orrections to the trajectories arise when a realistic attractive uclear potential is used.

In semiclassical formalism, it can be shown that [1]

$$\frac{P_{\rm tr}}{\sin(\theta_{\rm c.m.}/2)} \propto e^{-2\alpha D}. \tag{5}$$

Figure 8 shows the variation of experimental $P_{\rm tr}/\sin(\theta_{\rm c.m.}/2)$ as a function of D, obtained by using expressions (3) and (4) corresponding to large values of D, where uclear effects are expected to be minimum. It is seen from ig. 8 that there is an exponential dependence of $P_{\rm tr}$ on D as uggested by Eq. (5). The experimental data were fitted to an xponential function to derive the slope parameter α for varius transfer channels. The values of α are shown in Fig. 9 or all the systems as a function of the beam energy (in terms f $E_{\rm c.m.}/V_B$, where V_B is the Coulomb barrier). In the semilassical model, the slope parameter α depends on the averge binding energy E_b of the transferred particle through the elation $\alpha=\sqrt{2\mu E_b}/\hbar$. For proton and other higher charged ultinucleon transfer, one needs to apply corrections to the inding energy due to the Coulomb field ΔV of the collision artner and due to the Coulomb barrier V_c as given by [4]

$$E_b = E_b^{(0)} - \Delta V + V_c, \tag{6}$$

here $E_b^{(0)}$ is the uncorrected binding energy of the transerred particle(s). The Coulomb field ΔV was calculated corresponding to the average transfer distance parameter d = 1.555 fm. In calculating V_c, a radius parameter of $r_c=1.2$ fm has been used.

The calculated values of α for different transfer channels in all the three systems are shown in Fig. 9 by dashed lines. It is seen that in case of the $^{19}F+^{232}Th$ reaction, the experimental slope parameter for $1p$ transfer (α_{1p}) shows good agreement with the calculated values at all energies. How-

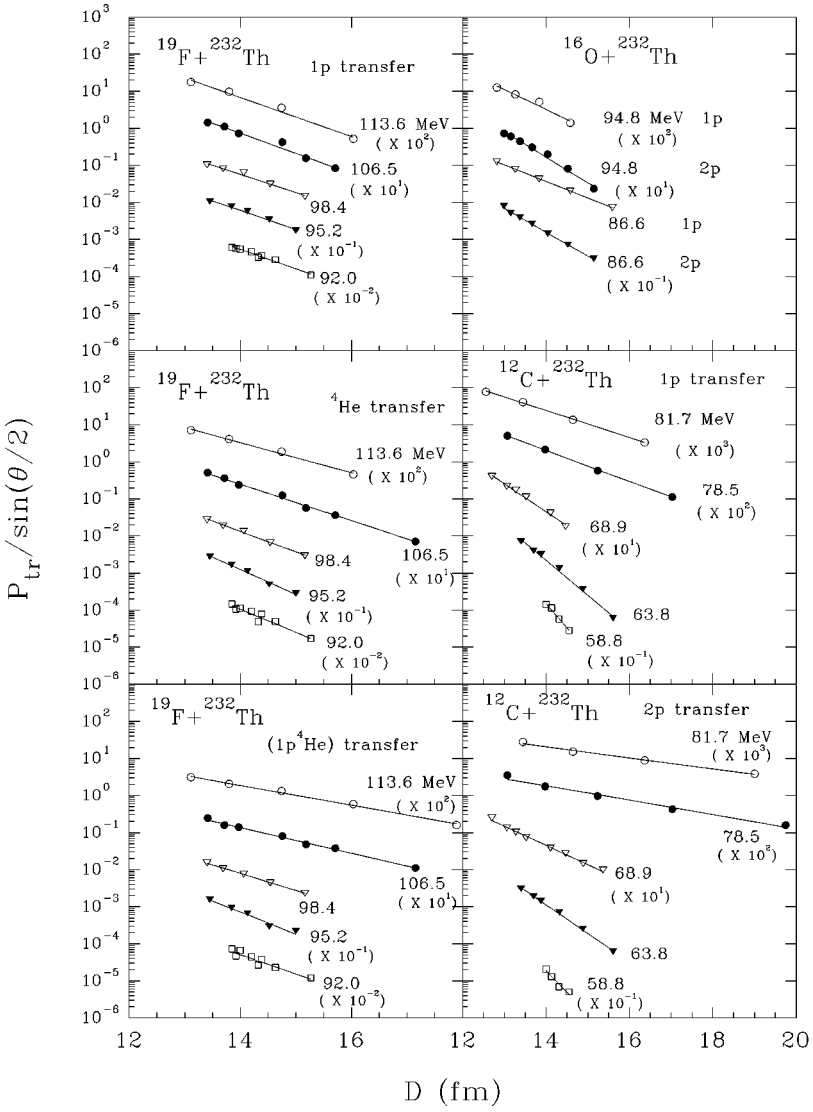

FIG. 8. Transfer probability vs distance of the closest approach for $1p$ and $2p$ transfer in the case of ^{16}O, ^{12}C+ ^{232}Th reactions and for $1p$, ^{4}He, and correlated (p^{4}He) transfer for the ^{19}F+ ^{232}Th system.

ever, the slope parameters for ^{4}He and (p^{4}He) transfer for this system do not agree with the estimated values of α at any energy. For ^{12}C+ ^{232}Th, and ^{16}O+ ^{232}Th systems the experimental slopes of $1p$ transfer (α_{1p}) are in reasonable agreement with the calculations at near-barrier and subbarrier energies, but show some deviation at higher energies. For $2p$ stripping channels in the case of ^{16}O, ^{12}C+ ^{232}Th reactions, the calculated slope parameters deviate largely from the experimental values, indicating the presence of slope anomaly in these reactions. It is also observed that the experimental slope parameters show a strong energy dependence in ^{12}C+ ^{232}Th reaction for both $1p$ and $2p$ transfer channels. The observation of a large slope anomaly in the multinucleon transfer channels for all the systems suggest that multistep processes could be important in these reactions, even at subbarrier energies.

IV. EXPLANATION OF THE SLOPE ANOMALY DUE TO NUCLEAR EFFECTS AT ABOVE BARRIER ENERGIES

Heavy ion collisions are characterized by two dominating features viz. (a) strong Coulomb interaction, especially below the Coulomb barrier and (b) strong absorption, especially above the Coulomb barrier. With the inclusion of nuclear potential, the classical deflection function becomes multivalued and there can be two or more impact parameters for a given scattering angle [23]. Recently, it has been reported [24] that the variation of one- and two-nucleon transfer probabilities with the distance of closest approach can be understood on the basis of semiclassical models if the contributions from the nuclear and Coulomb branches of the classical deflection function are considered for energies above the Coulomb barrier.

The interaction potential is assumed to consist of the Coulomb potential $V_C(r)$ and nuclear potential, $V_n(r)$. For a uniformly charged sphere of radius R_C, the Coulomb potential is given by [25]

$$V_C(r)=\frac{Z_1Z_2e^2}{2R_C}\left(3-\frac{r^2}{R_c^2}\right), \quad r\leqslant R_C, \tag{7}$$

$$V_C(r)=\frac{Z_1Z_2e^2}{r}, \quad r\geqslant R_C. \tag{8}$$

The real nuclear potential, usually of Woods-Saxon (WS) form, is written as

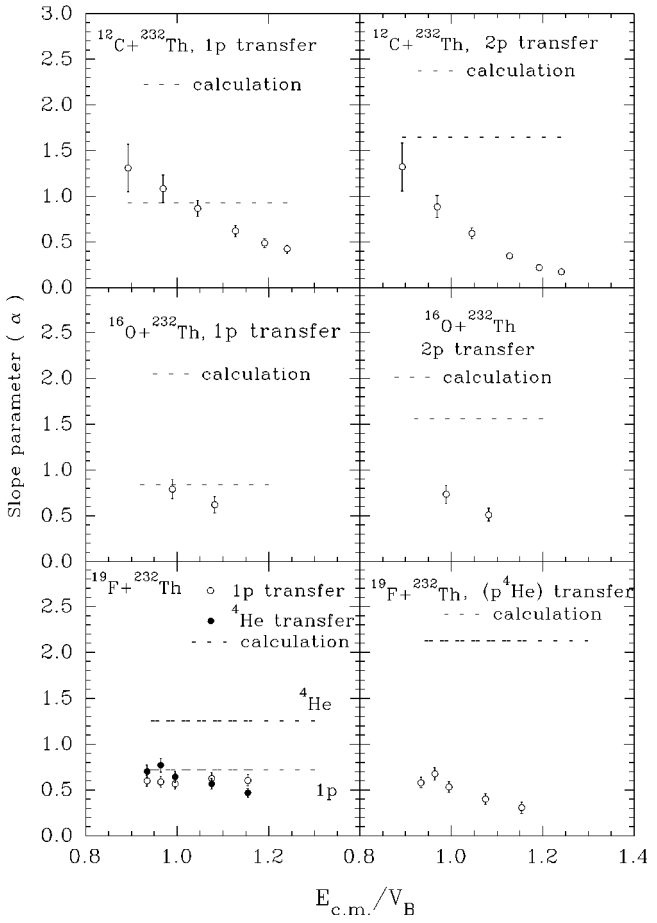

FIG. 9. Experimental slope parameter (α) plotted as a function of $E_{\text{c.m.}}/V_B$ for $1p$ and $2p$ transfer in the case of ^{16}O, ^{12}C+^{232}Th reactions and for $1p$, ^{4}He, and correlated (p^4He) transfer for the ^{19}F+^{232}Th system. The dashed lines are from semiclassical calculations.

$$V_n(r) = -V_0\left[1+\exp\left(\frac{r-R}{a}\right)\right]^{-1}. \tag{9}$$

By adding the centrifugal term, we obtain the effective potential

$$U_{\text{eff}}(b,r) = V_C(r) + V_n(r) + \frac{b^2E}{r^2}. \tag{10}$$

The deflection function is determined by the scattering potential using the classical expression

$$\Theta(b,E) = \pi - 2b\int_{r_{\min}}^{+\infty} dr\,\frac{1}{r^2}\left(1-\frac{U_{\text{eff}}(b,r)}{E}\right)^{-1/2}, \tag{11}$$

where $r_{\min}$ is the outermost turning point, i.e., the distance of closest approach (D) and is obtained from the solution of the equation

$$E_{\text{c.m}} - V_c(r) - V_n(r) - \frac{b^2E}{r^2} = 0. \tag{12}$$

The classical deflection angle as a function of D has been calculated and Fig. 10 shows the typical results of such a calculation for each system at two energies (above and below the Coulomb barrier). The parameters used for the real part of the nuclear potential having WS form were taken from the optical model analysis of the quasielastic data as described in

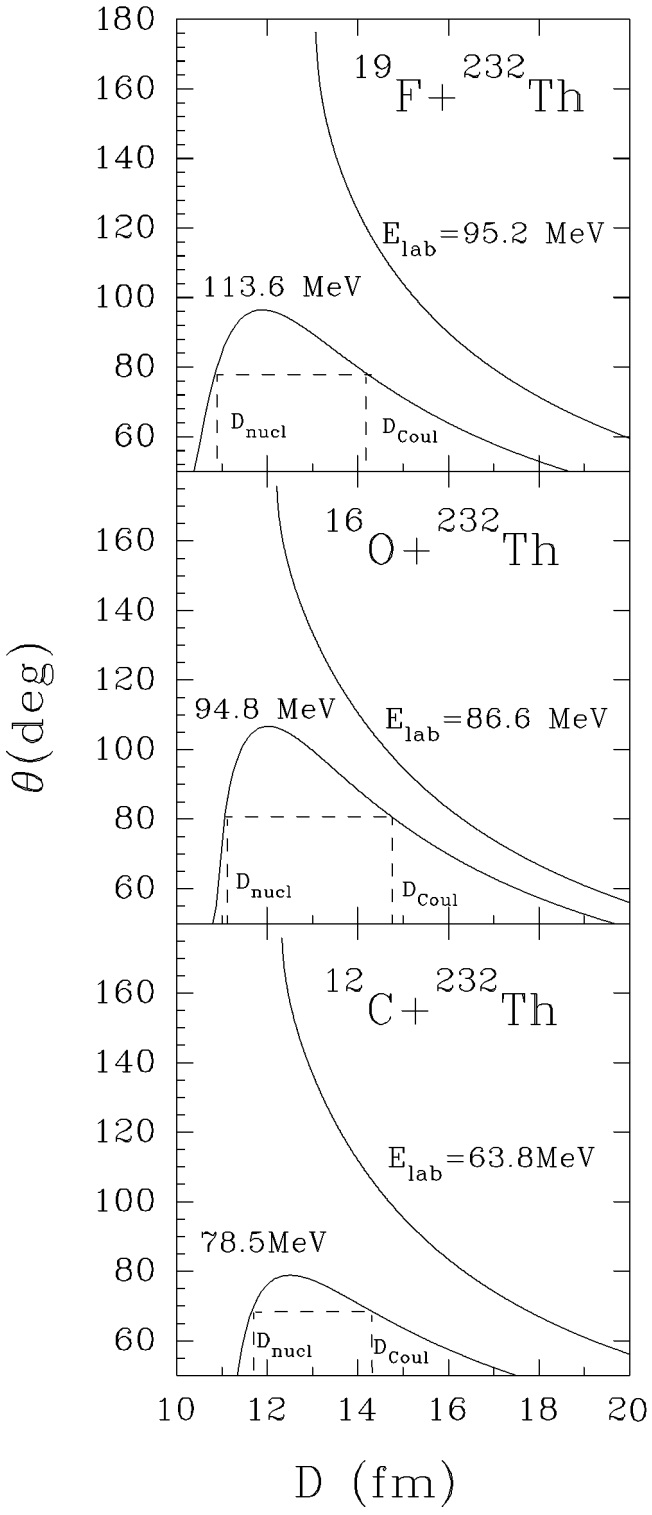

FIG. 10. Classical deflection angle vs distance of closest approach (D) for ^{12}C, ^{16}O, ^{19}F+^{232}Th. The Coulomb and nuclear branches of the distance of the closest approach corresponding to $\theta_{\text{c.m}}$ have been indicated for higher energies.

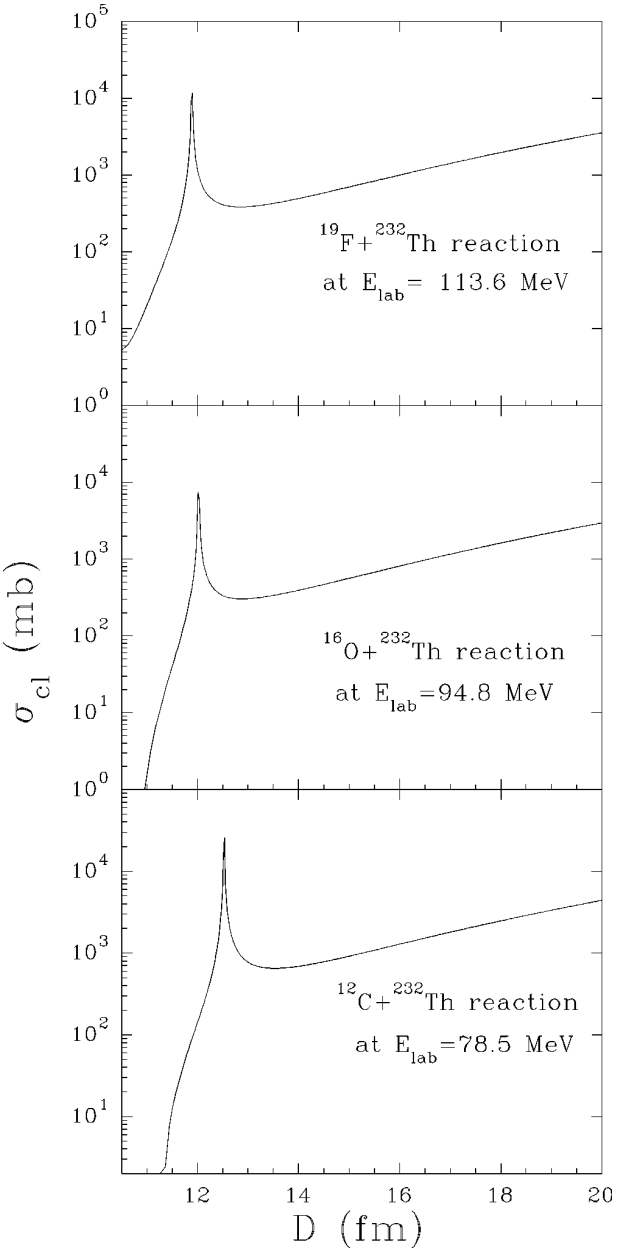

FIG. 11. Classical cross section (σ_{cl}) as a function of D for ^{12}C, ^{16}O, ^{19}F+^{232}Th at energies above the Coulomb barrier.

Sec. III B. For weak potentials, the inverse of the deflection function is single valued, i.e., for each scattering angle θ there is a unique impact parameter.

It is observed that for energies above the Coulomb barrier, the classical deflection function is multivalued for a given scattering angle and there can be two or more impact parameters and hence distances of closest approach. At energies very close to the Coulomb barrier and at subbarrier energies, the deflection function is single valued. The classical differential scattering cross section is given by

$$\sigma_{\rm cl}(b)=\frac{b}{\sin\theta}\left|\frac{db}{d\theta}\right|. \tag{13}$$

In Fig. 11 we have plotted the classical cross section (σ_{cl}) as a function of distance of closest approach D for the three systems at energies above the Coulomb barrier.

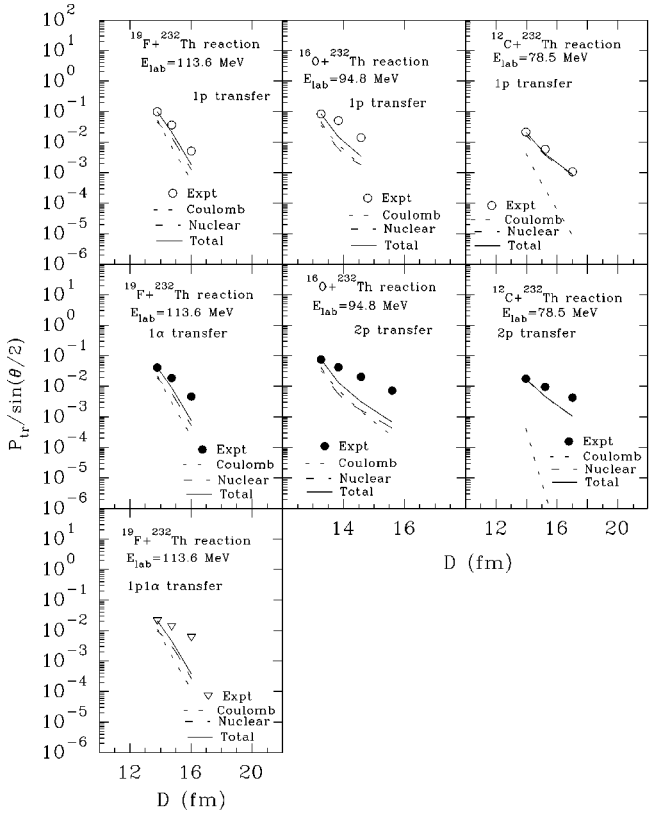

FIG. 12. Transfer probability vs the distance of the closest approach (D) for ^{12}C, ^{16}O, ^{19}F+^{232}Th reactions along with semiclassical calculations with and without nuclear effects. In the case of the ^{12}C+^{232}Th reaction the nuclear part merges with the total.

Considering the Coulomb and nuclear branches of the deflection function, the quasielastic (QE) scattering amplitude for a given angle is given by sum of the scattering amplitudes for these two branches:

$$a_{\rm QE}=a_{\rm QE}({\rm Coul})+a_{\rm QE}({\rm nucl}). \tag{14}$$

The QE scattering cross section is given by $|a_{\rm QE}|^2$. Similarly, the transfer cross section also arises from two branches and these are given by $\sigma_{\rm QE}(D_{\rm Coul})P_{\rm tr}(D_{\rm Coul})$ and $\sigma_{\rm QE}(D_{\rm nucl})P_{\rm tr}(D_{\rm nucl})$ where, $P_{\rm tr}(D_{\rm Coul})$ and $P_{\rm tr}(D_{\rm nucl})$ are the transfer probabilities and $D_{\rm Coul}$ and $D_{\rm nucl}$ are the distances of closest approach for the Coulomb and nuclear branches, respectively. The total transfer probability is then given by

$$P_{\rm tr}(D)=P_{\rm tr}(D_{\rm nucl})\frac{\sigma_{\rm QE}(D_{\rm nucl})}{\sigma_{\rm QE}}+P_{\rm tr}(D_{\rm Coul})\frac{\sigma_{\rm QE}(D_{\rm Coul})}{\sigma_{\rm QE}}. \tag{15}$$

Since $D_{\rm nucl}$ is less than $D_{\rm Coul}$, $P_{\rm tr}(D_{\rm nucl})$ is much larger than $P_{\rm tr}(D_{\rm Coul})$, especially for two-nucleon transfer reactions, because of its exponential dependence on D and due to the large value of α_{2p}.

In the semiclassical model the transfer probability, $P_{\rm tr}$, shows an exponential fall with the angle dependent distance of closest approach D and is expressed as

$$P_{\rm tr}(D)=P_{\rm tr}(D_0)\exp[-2\alpha(D-D_0)], \tag{16}$$

where D_0 is a scale parameter, taken as $D_0=1.4(A_P^{1/3}+A_T^{1/3})$ fm. In the present calculations, the contributions from the two branches are added incoherently. The transfer probability as a function of D was calculated using Eq. (15). A constant value of $P_{tr}(D)=P_{tr}(D_0)$ was used for $D<D_0$. The calculated transfer probability was normalized with the experimentally available value near D_0. The results are shown in Fig. 12 where the contributions from the Coulomb branch, nuclear branch, and total are shown along with the experimental values of P_{tr} as a function of D. The results are given at the higher energies to illustrate the calculations and it is seen that with inclusion of nuclear effects, the experimental data are better explained in all the reactions at above barrier energies. The inclusion of nuclear effects essentially reduces the value of α, bringing the calculated values closer to the experimental values. At below barrier energies, since the deflection angle as a function of D does not show multivalued behavior (as shown in Fig. 10), there are no corrections due to the nuclear effects in the calculation of slope parameter and the ''slope anomaly'' will still exist in the multinucleon transfer reactions at subbarrier energies.

V. SUMMARY AND CONCLUSIONS

In summary, we have measured the cross section of different transfer channels in the reactions of ^{19}F, ^{16}O, ^{12}C+^{232}Th at energies around the Coulomb barrier. The experimentally measured angular distribution data show the characteristic behavior of direct transfer reactions and the energy spectra are typically centered at energies corresponding to the optimum Q-values (Q_{opt}). The experimentally measured transfer cross section data have been compared with the total reaction cross section and it is found that the transfer yields are much higher in case of ^{19}F, ^{16}O + ^{232}Th reactions as compared to the ^{12}C+^{232}Th reaction at all energies. At subbarrier energies, there is a sharp increase in the relative cross section of transfer channels (σ_{tr}) in comparison to the total reaction cross section ($\sigma_{tr}+\sigma_{ff}$). The transfer probabilities derived from the cross section data show an exponential decrease with increasing distance of closest approach (D) at all energies for all the three systems. The experimental slope parameters obtained from the P_{tr} vs D plot were compared with semiclassical calculations. It is observed that the semiclassical picture is valid for $1p$ at near-barrier and subbarrier energies, whereas in case of $2p$, ^{4}He, and (p^4He) correlated transfers, the slope anomaly still persists, indicating the presence of strong nuclear effects and multistep processes in these reactions even at the subbarrier energies.

ACKNOWLEDGMENTS

The authors are thankful to Dr. S. S. Kapoor for many illuminating discussions and suggestions on this work, and to Dr. A. Saxena, L. M. Pant, and B. V. Dinesh for their help during the experiment. We also acknowledge help from Zafar Ahmed in some of the theoretical calculations. The assistance from the operation staff of the Pelletron accelerator is gratefully acknowledged.

[1] R. Bass, *Nuclear Reactions with Heavy Ions* (Springer, Berlin, 1980).
[2] J. F. Liang, L. L. Lee, Jr., J. C. Mohan, and R. J. Vojtech, Phys. Rev. C **47**, R1342 (1993).
[3] A. H. Wuosmaa *et al.*, Phys. Lett. B **255**, 316 (1991).
[4] L. Corradi *et al.*, Z. Phys. A **335**, 55 (1990).
[5] L. Corradi *et al.*, Phys. Rev. C **49**, R2875 (1993).
[6] D. C. Biswas, R. K. Choudhury, D. M. Nadkarni, and V. S. Ramamurthy, Phys. Rev. C **52**, R2827 (1995).
[7] D. M. Herrick, F. L. K. Wolfs, D. C. Bryan, C. G. Freeman, K. L. Kurz, D. H. Matthews, P. A. A. Perera, and M. T. Zanni, Phys. Rev. C **52**, 744 (1995).
[8] R. M. DeVries, Phys. Rev. C **8**, 951 (1973).
[9] T. Tamura *et al.*, Phys. Lett. **66B**, 109 (1977).
[10] T. Udagawa and T. Tamura, in *Continuum Spectra of Heavy Ion Reactions*, edited by T. Tamura, J. B. Natowitz, and D. H. Youngblood (Harwood Academic, Chur, Switzerland, 1980), p. 155.
[11] J. F. Liang, L. L. Lee, Jr., J. C. Mohan, and R. J. Vojtech, Phys. Rev. C **50**, 1550 (1994).
[12] C. Y. Wu *et al.*, Phys. Lett. B **188**, 25 (1987).
[13] S. Saha, Y. K. Agarwal, and C. V. K. Baba, Phys. Rev. C **49**, 2578 (1994).
[14] E. Vigezzi and A. Winther, Ann. Phys. (N.Y.) **192**, 432 (1989).
[15] C. V. K. Baba, V. M. Datar, K. E. G. Lobner, A. Navin, and F. J. Schindler, Phys. Lett. B **338**, 147 (1994).
[16] N. Majumdar, P. Bhattacharya, D. C. Biswas, R. K. Choudhury, D. M. Nadkarni, and A. Sexena, Phys. Rev. C **53**, R544 (1996); **77**, 5027 (1996).
[17] D. C. Biswas, M. N. Rao, and R. K. Choudhury, Nucl. Instrum. Methods Phys. Res. B **53**, 251 (1991).
[18] Y. Alhassid, R. D. Levine, J. S. Karp, and S. G. Steadman, Phys. Rev. C **20**, 1789 (1979).
[19] J. S. Karp, S. G. Steadman, S. B. Gazes, R. Ledoux, and F. Videbaek, Phys. Rev. C **25**, 1838 (1982).
[20] P. Schwandt, SNOOPY8Q optical model code, Indiana University report, 1984.
[21] J. P. Lestone, J. R. Leigh, J. O. Newton, and J. X. Wei, Nucl. Phys. **A509**, 178 (1990).
[22] C. Y. Wong, Phys. Rev. Lett. **31**, 766 (1973).
[23] R. A. Broglia and A. Winther, *Heavy Ion Reactions* (Addison-Wesley, Reading, MA, 1991), Vol. 1.
[24] B. K. Nayak, R. K. Choudhury, D. C. Biswas, L. M. Pant, A. Saxena, D. M. Nadkarni, and S. S. Kapoor, Phys. Rev. C **55**, 2951 (1997).
[25] W. E. Frahn, *Heavy-Ion High Spin States and Nuclear Structure* (IAEA, Vienna, 1975), Vol. 1, p. 157.